Journal of Asian Earth Sciences 138 (2017) 657–671

Contents lists available at ScienceDirect

Journal of Asian Earth Sciences

journal homepage: www.elsevier.com/locate/jseaes

Geochemistry of the dissolved loads of the Liao River basin in northeast China under anthropogenic pressure: Chemical weathering and controlling factors

Hu Ding, Cong-Qiang Liu *, Zhi-Qi Zhao, Si-Liang Li, Yun-Chao Lang, Xiao-Dong Li, Jian Hu, Bao-Jian Liu

State Key Laboratory of Environmental Geochemistry, Institute of Geochemistry, Chinese Academy of Sciences, Guiyang 550002, China

ARTICLE INFO

Article history:
Received 1 September 2015
Received in revised form 11 July 2016
Accepted 23 July 2016
Available online 1 December 2016

Keywords:
River water chemistry
Chemical weathering
CO_2 consumption
Liao River

ABSTRACT

This study focuses on the chemical and Sr isotopic compositions of the dissolved load of the rivers in the Liao River basin, which is one of the principal river systems in northeast China. Water samples were collected from both the tributaries and the main channel of the Liao River, Daling River and Hun-Tai River. Chemical and isotopic analyses indicated that four major reservoirs (carbonates (+gypsum), silicates, evaporites and anthropogenic inputs) contribute to the total dissolved solutes. Other than carbonate (+gypsum) weathering, anthropogenic inputs provide the majority of the solutes in the river water. The estimated chemical weathering rates (as TDS) of silicate, carbonate (+gypsum) and evaporites are 0.28, 3.12 and 0.75 t/km^2/yr for the main stream of the Liao River and 7.01, 25.0 and 2.80 t/km^2/yr for the Daliao River, respectively. The associated CO_2 consumption rates by silicate weathering and carbonate (+gypsum) weathering are 10.1 and 9.94 $\times$ 10^3 mol/km^2/yr in the main stream of the Liao River and 69.0 and 80.4 $\times$ 10^3 mol/km^2/yr in the Hun-Tai River, respectively. The Daling River basin has the highest silicate weathering rate (TDS_{sil}, 3.84 t/km^2/yr), and the Hun-Tai River has the highest carbonate weathering rate (TDS_{carb}, 25.0 t/km^2/yr). The Raoyang River, with an anthropogenic cation input fraction of up to 49%, has the lowest chemical weathering rates, which indicates that human impact is not a negligible parameter when studying the chemical weathering of these rivers. Both short-term and long-term study of riverine dissolved loads are needed to a better understanding of the chemical weathering and controlling factors.

1. Introduction

Geochemical investigations of large rivers provide important information about the biogeochemical cycles of the elements, the weathering rates, and CO_2 consumption by the acid degradation of continental rocks (Gaillardet et al., 1997). These results, in turn, provide insights into the Earth's surface dynamics and long-term climatic evolution (Kump et al., 2000; Chetelat et al., 2008; Goudie and Viles, 2012; Jin et al., 2014). Based on the chemical mass balance between the solid phase and the dissolved load of rivers, geoscientists have found that chemical weathering of silicates is the dominant long-term sink for atmospheric CO_2 and is thus the dominant regulator of the green-house effect over geological timescales (Raymo et al., 1988). However, the factors that control chemical weathering are complex and interrelated, and it is very difficult to isolate the contributions of any single factor (Goudie and Viles, 2012). Thus, the effects that these factors have on chemical weathering are still uncertain. More and better datasets on the chemical weathering rates across diverse of climates and lithology and on their controlling factors are needed to understand the links between silicate weathering and the global carbon cycle (Goudie and Viles, 2012) and to interpret and predict the past and future changes of the global climate (Chetelat et al., 2008; Moon et al., 2009).

In China, chemical weathering has been studied for river basins under subtropical climates and warm temperate climates (Han and Liu, 2004; Wu et al., 2005; Xu and Liu, 2007, 2010), but information on chemical weathering under temperate climates is poorly documented (Liu et al., 2013). The Liao River basin, which is located in a sub-humid temperate and warm-temperate zone, is the seventh largest river in China in terms of both its annual discharge and drainage area. The basin is characterized by geological diversity and is mainly covered by Quaternary deposits, volcanics, granites and carbonate rocks. Some rivers in the Liao River Basin are heavily

* Corresponding author at: Institute of Geochemistry, Chinese Academy of Sciences, 46 Guanshui Road, Guiyang 550002, China.
E-mail address: liucongqiang@vip.skleg.cn (C.-Q. Liu).

http://dx.doi.org/10.1016/j.jseaes.2016.07.026
1367-9120/

affected by human activities. For instance, the main stream of the Liao River was reported to be the second most polluted river among China's seven largest rivers (SEPA, 1996). Thus, this river basin offers the possibility of investigating chemical weathering and the different controlling factors under temperate climate. It is important to understand the dissolved load variations under anthropogenic pressure and water quality evolution in rivers (Roy et al., 1999; Chetelat et al., 2008; Raymond et al., 2008).

In this study, a systematic investigation of the water geochemistry (major ions and $^{87}Sr/^{86}Sr$ ratios) of the Liao River basin was carried out to (1) characterize the aqueous geochemistry and its controlling factors to decipher the different sources of the solutes, (2) quantify the rock weathering and associated CO_2 consumption rates, and (3) explore the mechanisms controlling chemical weathering within the Liao River Basin.

2. General setting of the study area

2.1. Geography and geology

The Liao River basin is located in the south of Northeastern China, lying between 116°54′–125°32′E longitude and 40°30′–45°17′N latitude. It covers a total area of 22.9×10^4 km^2 and includes two river systems: the Liao River system and the Hun-Tai River system. The two headstreams are the Xiliao River, which originates from Guangtou Mountain (alt. 1729 m) in Hebei Province, and the Dongliao River, which originates from Sahaling Mountain (alt. 360 m) in Jilin Province. After the confluence of these headstreams, the river is called the Liao River (the main stream) and finally flows into Liaodong Bay in the Bohai Sea (Fig. 1). The Hun-Tai River includes the Daliao River, Hun River, Taizi River and their tributaries. The Daliao River originates from Gunmaling Mountain, and the Taizi River originates from Hongshilizi Mountain. The Daliao River becomes a tidal river after the confluence of the Taizi River and finally flows into Liaodong Bay (Fig. 1). We also sampled the water of the Daling River located in the southwestern portion of the Liao River Basin. It is 397 km in length and covers a total area of 2.33×10^4 km^2, more than 1/6 of Liaoning Province. Its topography reduces from northwest to southeast, and it finally flows into Liaodong Bay (Fig. 1).

A simplified geological map is shown in Fig. 2. The Liao River Basin lies on the boundary of the North China Craton and the Xing'an-Mongolia Orogenic Belt (Yang et al., 2004). The central and northern parts of the Liao River basin are mainly distributed with Quaternary deposits (e.g., grit, silt, clay, breccia and gypsum-salt), beneath which the basement is composed of Paleozoic strata, granites and gneiss (Wu et al., 2001). The lower reaches of the Liao River and Hun-Tai River are similar. The upper reaches of the Xiliao River and the whole Daling River Basin are dominated by clastic rocks and volcanics, whereas the lithology of the upper reaches of the Dongliao River is dominated by granites and terrestrial clastic rocks (Fig. 2).

2.2. Hydrology, land cover and human activities

Governed by the sub-humid temperate and warm-temperate continental monsoon climate, the mountainous region of the Liao River Basin is colder than the plain region, with multi-year average, maximum and minimum temperature ranges of 4–9 °C, 20–30 °C, and −10 to −18 °C, respectively. The annual precipitation received by the basin is approximately 300–1000 mm and decreases progressively from the southeast to the northwest. The majority of the precipitation takes place during the flood season from June to September, accounting for approximately 75% of the annual precipitation (Li et al., 2012). Runoff from the Liao River basin is mainly distributed in the Hun-Tai River, which accounts for

Fig. 1. Sampling locations and land cover of Liao River and the Daling River basins. The land cover data were adapted from the Environmental and Ecological Science Data Center for West China, National Natural Science Foundation of China (http://westdc.westgis.ac.cn).

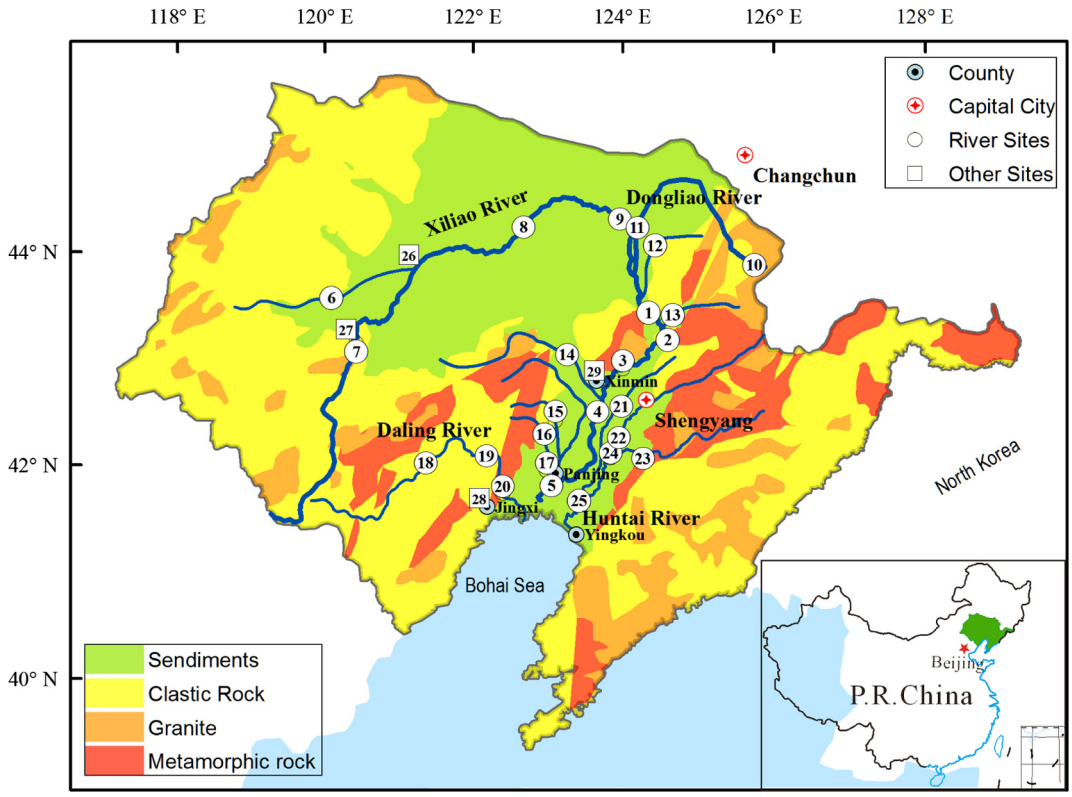

Fig. 2. Major rock types of the Liao River and the Daling River basins. Data adapted from the Simplified Geological Map of China (2012) (based on a 1:5,000,000 scale) provided by the China Geologic Survey (CGS).

approximately 45% of the total runoff, followed by the middle and lower reaches of the Liao River (28%). The Xiliao and Dongliao River have the lowest proportion, accounting for 21% and 6%, respectively (Table 1).

The Liao River basin is covered by mountains (48.2%), plains and lowlands (24.3%), hills (21.5%) and sandhills (6%). The upper reaches of the Xiliao River flow through mountain regions and Khorchin sandy areas, and the lower reaches flow through an alluvial plain. For the Dongliao River, the upper reaches are distributed in hills with good vegetation cover, and the middle and lower reaches are mainly distributed in an alluvial plain. The Daling River flows through mountains, hills and piedmont clinoplain from upstream to downstream. In the middle and lower reaches of the Liao River is the Liaohe plain. Land use in the Liaohe plain is complex, with approximately half of the region affected by agricultural activities. In the rest of the area, water bodies, residential buildings, grassland and forest dominate (Qin et al., 2013).

There is 4.95×10^4 km^2 of agricultural land in the Liao River basin, most of which is located in the middle and downstream areas. Approximately 10% of the agricultural land is paddy fields, which are mainly located in the downstream portions of the Liao and Dongliao Rivers (Li et al., 2012). A previous study showed that waste effluents are a major contributor of nitrogen in these rivers in the middle and lower reaches (Yue et al., 2013), suggesting direct anthropogenic inputs for these rivers. The Liao River basin is a developed region and is the manufacturing, grain production and animal husbandry base of China. The population density of the Liao River basin is higher than the averages for both the Northeastern Region of China (82 indiv./km^2) and the whole country (135 indiv./km^2) (Table 1). Industrial waste water, urban sewage discharged, and the agricultural non-point source pollution made the Liao River one of the most polluted river of China in 1990s. The pollutants includes ammonia, volatile phenol (SEPA, 1996). Although noticeable improvement in recent years, water quality safety of the basin is still a key issue of the state and local government (Song, 2015). Hundreds of water conservancy projects, serving to water supply, hydroelectric power, flood control, irrigation, etc, have been setup during the past 60 years in the basin (For instance, the number of reservoirs with the capacity bigger than 10^6 m^3 in Liao River basin increased from 2 in 1949 to 85 in 1988), and were reported to be one major reason of water discharge and sediment load variations of Liao River system (Liu et al., 2007).

Table 1
General information of each river in the study area.

Rivers	Length (km)	Area (10^4 km^2)	Discharge (10^8 m^3/yr)	Population density (indiv./km^2)[b]
Liao River[a]	1345	22.9	126	153
Xiliao River	827	13.2	26.7	57
Dongliao River	372	1.02	8.36	243
Hun-Tai River	–	2.73	66.2	–
Daling River	397	2.33	17.6	280

[a] Drainage area and annual discharge of the Hun-Tai River are included, but the length is only for the Liao River.
[b] Average population density of each basin. Date source: Yan et al. (2000) for Liao River, Zhao (2011) for Xiliao River, Xia et al. (2009) for Dongliao River, the data of Daling River comas from EPBLP (2011).

The upper reaches flow through mountain areas with good vegetation cover and are subjected to less industrial or domestic pollution. However, waters of the middle and lower reaches face pollution problems. Generally, pollution in the Dongliao River is heavier than that in the Xiliao River, and the lower reaches are more polluted than the upper reaches are. Within the Hun-Tai River system, the Taizi River is the most polluted (Li et al., 2012; Yue et al., 2013). Industrial waste water, urban sewage discharge, and agricultural non-point source pollution have made the Liao River one of the most polluted rivers in China (SEPA, 1996).

3. Sampling and analytical methods

The main streams of the Liao River, Hun-Tai River and Daling River, as well as their major tributaries, were sampled during July 2010. The sampling locations together with the spatial distribution of TDS concentration are shown in Fig. 1. Samples were collected from the river bank at depths ranging from 50 cm to 100 cm or from the middle of the river when a boat was available. In total, 25 river water and 2 other water (rainwater and sewage water) samples were collected and presented in this study.

For each sample, 10–20 L of water was collected using high density polyethylene (HDPE) containers that had previously been acid-washed and cleaned with ultrapure water. Water samples were filtered for a few hours after sampling through pre-washed 0.22 μm Millipore membrane filters. The first liter of the filtration was discarded to clean the filter, and then a small volume was stored for anion analysis. Another portion was acidified with ultra-pure 6 M HCl to pH < 2 and stored separately in HDPE bottles (pre-washed with double-distilled ultra-purified HCl and rinsed with Milli-Q 18.2 MΩ water) to measure the cations and the $^{87}Sr/^{86}Sr$. All of the samples were sealed and kept in the dark.

The temperature, pH and electric conductivity (EC) were measured on site using a portable EC/pH meter (WTW, pH 3210/Cond 3210 Germany), and the alkalinity was determined by titration with HCl before filtration. The accuracies were ±0.01, ±0.1 (°C), ±0.5% and ±0.01 (ml) for the determination of pH, temperature, EC and the amount of HCl consumed in the titration of alkalinity, respectively. The concentrations of major cations (Ca^{2+}, Mg^{2+}, Na^{+}, K^{+}) and silica were measured by Inductively Coupled Plasma Optical Emission Spectrometry (ICP-OES, Vista MPX, USA) with a precision better than 5%. Anion (Cl^{-}, NO_3^{-} and SO_4^{2-}) concentrations were determined by ionic chromatography (Dionex, ICS-90, USA) with a precision of 5%. Regent and procedural blanks were determined in parallel to the sample treatment and the national standard reference materials of China were used in the determination of cations and anions.

The Sr isotopic ratios ($^{87}Sr/^{86}Sr$) were measured by Multi collector-Inductively Coupled Plasma-Mass Spectrometer (MC-ICPMS, Nu Plasma, UK) (Lang et al., 2006) after chromatographic separation on cationic exchange resin (Blum and Erel, 1997). The accuracy of the measurement was checked by running the NIST 987 standard, which yielded a mean $^{87}Sr/^{86}Sr$ ratio of 0.710268 ± 0.000008 ($2\sigma_{error}$, n = 35). Then, 6 samples were randomly selected for the determination of $^{87}Sr/^{86}Sr$ isotope ratio by TIMS (Thermal Ionization Multicollector Mass Spectrometry, IsoProbe-T, GV Instruments, England) for data quality control. There was good linearity between the groups of results, as determined by the two methods ($R^2 = 0.9992$, $y = 1.0004x - 0.0003$).

4. Results

4.1. Chemical compositions

The measured parameters (temperature, pH and EC) and concentrations of the major element of the samples are listed in Table 2. The river waters are alkalescent with pH ranging from 7.14 (sample 13) to 9.80 (sample 8) and an average pH of 8.11. The Xiliao River has the highest average pH of 8.81, whereas those of the Dongliao River and Hun-Tai River are lower, with mean values of 7.80 and 7.96, respectively. The EC of the water samples generally rangees from 254 μs/cm (sample 16) to 1304 μs/cm (sample 1), with an average of 526 μs/cm. The only exception was sample 5; it had high element concentrations: $[Cl^{-}]$ = 49,782 μmol/L, $[Ca^{2+}]$ = 4362 μmol/L, $[Mg^{2+}]$ = 5904 μmol/L, $[Na^{+}]$ = 30,225 μmol/L, $[K^{+}]$ = 540 μmol/L. These values are probably affected by sea water.

The total dissolved solid (TDS, mg/L), expressed here as the sum of major inorganic species concentrations ($Na^{+} + K^{+} + Ca^{2+} + Mg^{2+} + HCO_3^{-} + Cl^{-} + SO_4^{2-} + NO_3^{-} + SiO_2$), is also given in Table 2. For all of the river water samples except sample 5 (TDS = 3025 mg/L), the TDS values ranged from 170 (sample 13) to 861 mg/L (sample 12), with an average of 400 mg/L. This value is much higher than the global average value (100 mg/L, (Gaillardet et al., 1997) and is comparable to those of heavily polluted rivers such as the Seine (460 mg/L) in Paris (Roy et al., 1999), the Danube (428 mg/L) in Europe and the Nile (388 mg/L) in Africa (Gaillardet et al., 1999). The TDS values were lower than that observed in the Huai River (509 mg/L, (Zhang et al., 2011)) of China. Among the tributaries, the Xiliao River has the highest TDS value (averagely 545 mg/L), and the Daling River (averagely 495 mg/L) is in the same order of magnitude. The Hun-Tai River system and the Dongliao River have average TDS values of 311 mg/L and 305 mg/L, respectively (Fig. 1). The total dissolved cations ($TZ^{+} = K^{+} + Na^{+} + Ca^{2+} + Mg^{2+}$, in μEq/L) range from 2449 to 10,088 μEq/L (except sample 5, 51,300 μEq/L), with an average of 5196 μEq/L, which is four times higher than the estimated average of world rivers [TZ^{+} = 1125 μEq/L, (Meybeck, 2003)]. There is a significant linear correlation between TDS and TZ^{+} ($R^2 = 0.97$, excluding sample 5). The extent of inorganic charge imbalance, characterized by the normalized inorganic charge balance [$NICB = (TZ^{+} - TZ^{-})/TZ^{+}$, where $TZ^{-} = HCO_3^{-} + Cl^{-} + SO_4^{2-}$ in μEq/L], is within ±10% for most of the samples.

For the river water samples, the Na^{+} concentration is remarkably high, ranging from 376 (sample 13) to 6613 μmol/L (sample 9) with an average of 1892 μmol/L (except sample 5). This value is higher than that of the Huai River (1080 μmol/L) in China (Zhang et al., 2011) and is approximately two times higher than the world average value (928 μmol/L) and is similar to that of the Krishna River (1848 μmol/L) in south India (Gaillardet et al., 1999). The Xiliao River has the highest Na^{+} concentrations (an average of 3297 μmol/L), followed by the Daling River (averagely 2168 μmol/L). The Liao River main stream, the Dongliao River and the Hun-Tai River system have similar Na^{+} concentrations, with averages of 1062 μmol/L, 1075 μmol/L and 1093 μmol/L, respectively. Another common cation is Ca^{2+}, with concentrations ranging from 238 (sample 9) to 1849 μmol/L (sample 12) and an average value of 956 μmol/L. Among the anions, bicarbonate is dominant, with concentrations ranging from 934 (sample 13) to 6372 μmol/L (sample 7) and an average of 2816 μmol/L. The concentration of Cl^{-} ranges from 234 (sample 14) to 4477 μmol/L (sample 17), with an average of 1390 μmol/L (except sample 5).

Ternary diagrams were employed to illustrate the variations in the major cation, anion-Si and anion compositions of river water (Fig. 3). The samples defined a relatively wide range of values on the ternary diagrams, and most samples clustered toward the $K^{+} + Na^{+}$ apex (Fig. 3a) and the HCO_3^{-} apex (Fig. 3b). In the cation ternary diagram, some samples are within the value ranges of Songhuajiang River (Liu et al., 2013), and are somewhat similar as that of the Huanghe (Yellow River) (Gaillardet et al., 1999), but are distinct from those of Nanpanjiang and Beipanjiang River (Xu et al.), Wujiang River and Chanjiang (Yangtez) River

Table 2
The chemical compositions of major ions in the river waters from the Liao River basin and the Daling River basin, NE China (units: μmol/L).

Rivers	Sample				pH	EC (μs/cm)	Ca	Mg	Na	K	HCO_3	SO_4	Cl	NO_3	SiO_2	TDS (mg /L)	Sr	$^{87}Sr/^{86}Sr$	TZ^+ (μEq /L)	TZ^- (μEq /L)	NICB (%)
	No.	Date (MM/DD)	Longitude	Latitude																	
The Liao River main stream																					
Liao River	1	0707	123.654	42.614	8.71	1304	827	592	2112	121	2457	672	1774	4.87	49.5	381	4.00	0.709568	5072	5576	−9.9
	2	0710	123.837	42.329	7.84	323	811	389	642	97.1	1369	432	616	161	75.1	222	3.26	0.709277	3139	2850	9.2
	3	0709	123.186	42.138	8.30	371	918	426	683	100	1474	504	689	156	75.1	244	2.36	0.709314	3469	3172	8.6
	4	0709	122.763	41.785	7.94	437	866	467	809	112	1615	526	821	53.0	9.48	251	2.29	0.709647	3587	3488	2.8
	5	0708	122.043	41.170	8.23	6300	4362	5904	30,225	540	1545	1293	49,782	37.9	82.7	3025	16.8	0.709560	51,299	53,912	−5.1
Tributaries of Liao River																					
Xilamulun River	6	0709	119.576	43.251	8.16	541	1177	1064	1771	122	5319	634	667	0.84	214	540	5.38	0.709896	6374	7254	−13.8
Laoha River	7	0709	119.781	42.833	7.83	663	1331	1162	2578	30.7	6372	714	965	51.1	384	659	8.71	0.709807	7595	8765	−15.4
Xiliao River	8	0708	122.232	43.623	9.80	318	250	580	2224	30.7	2969	327	563	0.26	125	316	2.67	0.709925	3915	4186	−6.9
	9	0707	123.513	43.533	9.45	800	238	644	6613	34.4	5890	508	2135	16.4	29.0	665	2.52	0.709963	8412	9042	−7.5
Dongliao River	10	07010	125.152	42.892	7.74	308	820	344	491	105	1510	321	542	83.2	104	210	2.85	0.708959	2924	2693	7.9
	11	0707	123.723	43.423	7.86	497	1054	529	1659	114	3141	564	1342	59.8	101	401	4.03	0.709436	4939	5611	−13.6
Zhaosutai River	12	0707	123.906	43.227	8.19	1042	1849	627	4834	301	5480	962	3662	1316	179	861	8.15	0.709420	10,088	11,067	−9.7
Qing River	13	0707	123.962	42.549	7.14	504	698	296	376	84.6	934	378	387	182	84.5	170	3.05	0.708524	2449	2076	15.2
Liu River	14	0709	122.508	42.365	7.75	373	931	417	778	85.4	2598	274	234	77.4	91.6	272	2.60	0.709940	3561	3380	5.1
Dongsha River	15	0708	122.207	41.765	7.45	459	1306	1221	2251	74.1	3756	912	2952	0.95	110	564	6.19	0.709676	7378	8532	−15.6
Yangchang River	16	0708	122.032	41.662	8.33	254	696	637	2162	24.0	1896	720	1362	112	65.6	338	2.87	0.712861	4853	4698	3.2
Raoyang River	17	0708	121.974	41.270	7.66	371	983	860	3443	171	1685	718	4477	10.4	19.7	478	3.00	0.709981	7300	7598	−4.1
Daling River																					
	18	0710	120.466	41.577	8.22	325	779	843	877	65.4	2619	419	815	24.4	69.8	309	2.42	0.710447	4187	4273	−2.1
	19	0710	121.255	41.551	8.15	494	999	851	1646	104	2909	832	1312	67.2	123	418	4.19	0.709747	5449	5885	−8.0
	20	0710	121.383	41.179	8.17	824	1821	979	3981	151	4605	1582	3106	210	148	759	6.47	0.710062	9732	10,874	−11.7
The Hun-Tai River system																					
Pu River	21	0708	122.746	41.508	9.52	537	932	620	1582	199	2493	576	1562	27.2	1.91	361	2.44	0.711713	4885	5207	−6.6
Hun River	22	0708	122.821	41.374	7.44	467	1021	441	1141	125	1545	675	1070	360	106	308	2.16	0.713126	4189	3965	5.3
Taizi River	23	0708	123.217	41.252	7.45	406	876	411	687	149	1580	675	535	332	77.9	272	2.91	0.717042	3411	3464	−1.6
	24	0708	122.871	41.359	7.45	475	895	471	815	152	1755	780	635	315	82.2	301	3.32	0.716601	3698	3950	−6.8
Daliao River	25	0708	122.413	40.998	7.92	536	864	482	1242	160	1615	756	1145	264	56.0	312	2.23	0.714238	4096	4272	−4.3
Other types of water																					
Rainwater of Jinzhou city	28	0710			—	—	319	27.4	5.76	2.82	—	55.6	18.5	27.5	3.72	—	—	—	702	—	—
Wastewater from Xinmin city	29	0709			7.65	—	2407	1200	3560	234	8461	390	3672	1356	346	1005	7.10	0.709792	11,009	12,912	—

TDS: total dissolved solid.
NICB = 100%×(TZ^+-TZ^-)/TZ^+.

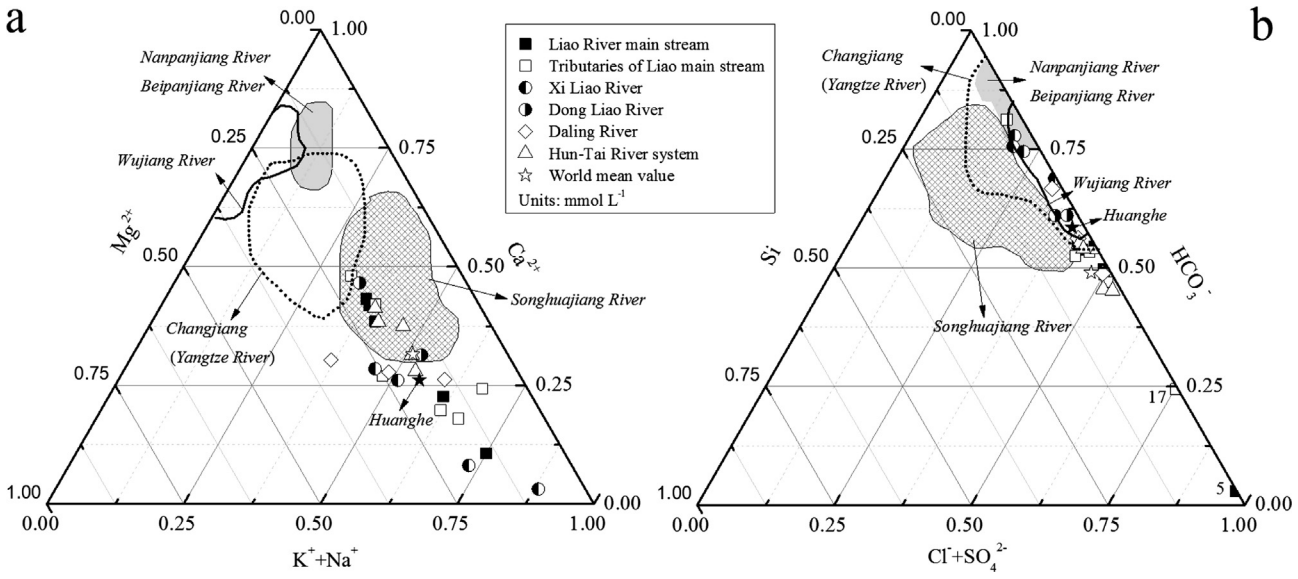

Fig. 3. Ternary diagrams showing cation (diagram a) and anion-Si compositions (diagram b). Also shown are chemical compositions of major ions from the large rivers in China for comparison. *Data sources:* Han and Liu (2004) (Wujiang), Xu and Liu (2007) (Nanpanjiang and Beipanjiang), Chetelat et al.(2008) (Changjiang), Gaillardet et al. (1999) (Huanghe and the world mean value), and Liu et al. (2013) (Songhuajiang River).

(Chetelat et al., 2008), which all dominated by carbonate weathering. For all of the river water samples, Ca^{2+} is the most abundant cation, accounting for 39% (average percentage, in μEq/L) of the total cations (TZ^+). The next most common are Na^+ and Mg^{2+}, accounting for 34% and 25% of TZ^+, respectively. K^+ made up the smallest proportion of the cations (2%). On the anion ternary diagram, our samples are within the range of the Wujiang River (Han and Liu, 2004), and are also somewhat similar as that of the Huanghe (Yellow River) (Gaillardet et al., 1999), but is distinct from the Songhuajiang River with less anthropogenic inputs (Liu et al., 2013). As the dominant anion, HCO_3^- accounts for 48% of the total anions (TZ^-), followed by Cl^- and SO_4^{2-}, which accounts for 26% and 24%, respectively.

4.2. Strontium concentration and isotope ratios

As shown in Table 2, with the exception of sample 5 (Sr = 16.8 μmol/L), the Sr concentrations of the Liao River, Daling River and their tributaries fall within a range between 2.16 (sample 2, Hun River) to 8.71 μmol/L (sample 7, Laoha River), with an average of 3.75 μmol/L. This value is four times higher than the global average of 0.89 μmol/L (Palmer and Edmond, 1992). The Xiliao River and the Daling River have the highest Sr concentrations with the averages of 4.82 and 4.36 μmol/L, respectively. The Sr isotopic composition ($^{87}Sr/^{86}Sr$) is fairly variable within the study area, ranging from 0.70852 (sample 13, Qing River) to 0.71704 (sample 23, Taizi River), with an average of 0.71075 (including sample 5,

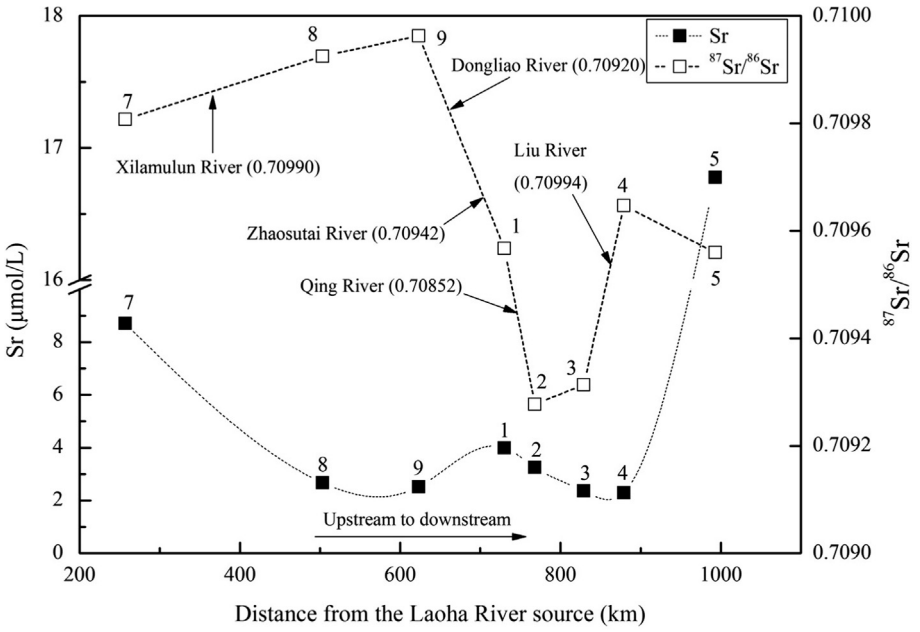

Fig. 4. Evolution of the Sr concentrations and $^{87}Sr/^{86}Sr$ ratios measured along the Liao River from the Laoha River source. Figures beside the square are sample numbers and in brackets are the $^{87}Sr/^{86}Sr$ ratios of the selected tributaries. Arrows show the location where the tributaries join.

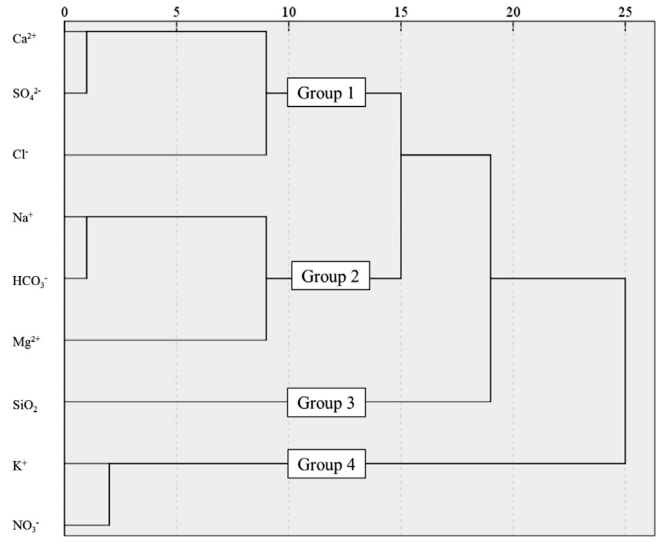

Fig. 5. Dendogram from the HCA (hierarchical cluster analysis) for the cation and anion concentrations of the river water samples (9 variables, units: μmol L^{-1}).

the downstream Liao River), which is lower than that of the global runoff and major rivers (Gaillardet et al., 1999). The $^{87}Sr/^{86}Sr$ ratios of the samples from the Xiliao River, Dongliao River and Liao River main stream are relatively constant, with averages of 0.70990, 0.70920 and 0.70957, respectively. The Hun-Tai Rivers had the highest $^{87}Sr/^{86}Sr$ ratio, with a mean of 0.71454.

The evolution of Sr concentration and the $^{87}Sr/^{86}Sr$ ratio from upstream to downstream in the Liao River system is shown in Fig. 4. The downstream evolution clearly reflects the geological setting of the Liao River basin. The rivers with draining areas that consist mainly of Quaternary sediments have low $^{87}Sr/^{86}Sr$ ratios and high Sr concentrations, whereas those draining the volcanic and granitic areas have high $^{87}Sr/^{86}Sr$ ratios and low Sr concentrations (Palmer and Edmond, 1992). As shown in Fig. 4, the Sr isotope ratios increase from 0.70981 to 0.70992 with the confluence of the Xilamulun River (0.70990). After the confluence of the Dongliao River (0.70920) and the Zhaosutai River (0.70742), the $^{87}Sr/^{86}Sr$ ratio decreases to 0.70957 and to 0.70928 after the impact of Qing River (0.70852). After that, it rises due to the effect of the Liu River (0.70994).

4.3. Statistical analysis

To study the chemical relationships among the variables of the river water samples, statistical techniques, such as cluster analysis, can be used as a powerful tool to analyze water-chemistry data and can be helpful in generating hypotheses for the sources of the observed geochemical phenomena (Güler et al., 2002). Cluster analysis has been successfully applied in many studies for the classification of water samples. In this study, the hierarchical cluster analysis (HCA, R-mode) was used to classify the variables of the river water samples into distinct hydrochemical groups based on correlations between the samples. The method is not fully described here, but a detailed explanation of the method was presented by Güler et al. (2002). The dendogram from the HCA for the cations and anions of the 24 river water samples (sample 5 was excluded due to its extremely high values) is shown in Fig. 5. The 9 variables monitored in the water samples were classified into 4 major groups: Group 1: Ca^{2+}, SO_4^{2-} and Cl^-; Group 2: Na^+, HCO_3^- and Mg^{2+}; Group 3: SiO_2; Group 4: K^+ and NO_3^-. Within the groups, SO_4^{2-}, Ca^{2+} in Group 1 and Na^+, HCO_3^- in Group 2 formed subgroups, indicating that the correlation between them is more significant than is the correlation with other variables in their groups and might have similar sources. Considering the geological background of the samples, Groups 1, 2 and 3 in the HCA analysis can be attributed to the dissolution of evaporites, carbonate and silicate, respectively. For Group 4, the anthropogenic and biological sources fit well with the HCA results because synthetic fertilizer and biomass can be rich in K^+ and NO_3^- and are considered to be two important sources of these ions in aquatic environments. Correlations among pH, EC, TDS and major ions were examined for the 24 river water samples (Table 3). TDS has a significant positive correlation ($p < 0.01$) with all of the cations and anions, with the exception of K^+ and NO_3^-. Bicarbonate has an obvious positive correlation ($p < 0.01$) with Mg^{2+} and Na^+, whereas NO_3^- significantly correlates with Ca^{2+} and K^+. Significant positive correlations ($p < 0.05$) are also observed between Cl^- and each of the cations. For the dissolved SiO_2, a significant positive correlation is observed with Mg^{2+}, HCO_3^- ($p < 0.01$) and Ca^{2+} ($p < 0.05$).

5. Discussion

5.1. Sources of solutes and end-member identification

5.1.1. Atmospheric input

Correcting for atmospheric input is the first step in deciphering the contributions of different sources to the solutes of river water. As shown in many studies, chloride is the most useful reference for evaluating the atmospheric input into rivers due to its conservative properties and the fact that it is not involved in biogeochemical cycling, except in small basins, where biota plays a dominant role (Gaillardet et al., 1997; Roy et al., 1999; Xu and Liu, 2007). Generally, three complementary methods can be used to correct for

Table 3
Pearson correlation matrix for pH, EC, TDS and major ions of the river waters in the study area.

	pH	EC	Ca^{2+}	Mg^{2+}	Na^+	K^+	HCO_3^-	SO_4^{2-}	Cl^-	NO_3^-	SiO_2	TDS
pH	1											
EC	0.235	1										
Ca^{2+}	−0.375	0.375	1									
Mg^{2+}	0.079	0.189	0.453*	1								
Na^+	0.449*	0.554**	0.184	0.428*	1							
K^+	−0.134	0.380	0.587**	−0.127	0.116	1						
HCO_3^-	0.325	0.505*	0.398	0.684**	0.732**	−0.020	1					
SO_4^{2-}	−0.121	0.446*	0.736**	0.519**	0.442*	0.401	0.372	1				
Cl^-	0.067	0.425*	0.490*	0.480*	0.719**	0.452*	0.353	0.626**	1			
NO_3^-	−0.183	0.355	0.522**	−0.203	0.244	0.708**	0.153	0.327	0.296	1		
SiO_2	−0.165	0.174	0.489*	0.522**	0.130	−0.125	0.647**	0.241	−0.058	0.175	1	
TDS	0.204	0.605**	0.618**	0.684**	0.850**	0.282	0.882**	0.675**	0.714**	0.377	0.486*	1

* Correlation is significant at the 0.05 level (two-sided).
** Correlation is significant at the 0.01 level (two-sided).

Table 4
The a priori end-member composition used in the inverse calculation.

A priori	Cl/Na	HCO_3/Na	K/Na	Ca/Na	Mg/Na	Sr/Na	$^{87}Sr/^{86}Sr$
Atmosphere (*marine aerosol*)	1.2 ± 0.1	–	0.02 ± 0.001	0.02 ± 0.01	0.11 ± 0.02	0.0002 ± 0.00001	0.709 ± 0.001
Anthropogenic (*for samples 2, 4, 11*)	5 ± 1	–	2 ± 1	–	–	–	–
Anthropogenic (*for samples 17, 20, 25*)	1 ± 0.5	–	0.17 ± 0.1	–	–	–	–
Carbonate (*+gypsum*)	–	100 ± 20	–	70 ± 20	25 ± 5	0.075 ± 0.01	0.708 ± 0.001
Evaporite (*halite*)	1 ± 0.001	–	–	–	–	0.003 ± 0.002	0.708 ± 0.001
Silicate	–	2 ± 1	0.17 ± 0.07	0.35 ± 0.15	0.24 ± 0.05	0.003 ± 0.001	0.73 ± 0.02

See text for details.

atmospheric input. First, if the river does not drain saline formations and the effect of human activities can be neglected, river water samples with the lowest chloride concentration are assumed to have obtained their dissolved [Cl^-] exclusively from an atmospheric origin (Meybeck, 1983; Viers et al., 2001). Then, other atmospheric elements can be corrected, depending on the ratio of their concentrations to those of Cl in the rain water. This approach for estimating the atmospheric contribution has the advantage that it does not require corrections for evapotranspiration if the samples are collected at the same time because its effect is already factored in by determining the chloride abundance of rivers (Rai et al., 2010). In addition, this method simultaneously corrects the inputs of other element from dry deposition. The second method consists of dividing the mean chloride concentration in rainwater by the evapo-transpiration factor (f_{et}), which is calculated as the ratio of the annual discharge over the annual precipitation received by the basin (Moquet et al., 2011). For this method, it is assumed that all of the inputs of the major elements from rain remain in the river water. Third, if the residence time of the river water is very short, the mean chloride concentration in the rain water could be used directly as the atmospheric input of [Cl^-], and the evapo-transpiration effect can be neglected (Shin et al., 2011).

In our study area, atmospheric input correction were applied separately for each of the following subregions: the Xiliao River, the Dongliao River, the Hun-Tai River, and the main streams of both the Liao River and the Daling River. Using the annual precipitation and evaporation data reported by (Qian, 2007), the f_{et} values for the regions mentioned above were calculated to be 0.05, 0.14, 0.33 and 0.17, respectively. In particular, the f_{et} for the Xiliao River basin is very low, with an annual discharge of 26.7×10^8 m^3, only approximately 5.5% of the annual precipitation received (489×10^8 m^3). Atmospheric input was corrected using the [Cl^-] concentration in the rainwater and the Cl-normalized ratio of the seawater (Li and Li, 1996; Wang et al., 1997; Liu, 2008; Wang and Xu, 2009; Chai et al., 2010). According to several studies (Gaillardet et al., 2003; Millot et al., 2003; Moon et al., 2009), the elemental ratios in seawater were used as the atmospheric end-member in the inversion calculation. The NO_3/Na molar ratio of rainwater was assumed to be 1.2, which is same as that of Liaozhong City (Chai et al., 2010), Primorskaya (Russia), and Kanghwa (Republic of Korea), as reported by EANET (Acid Deposition Monitoring Network in East Asia, http://www.eanet.cc).

5.1.2. Anthropogenic input

The population density of the study area is relatively high for the part of Liao River basin that lies in the Liaoning province at 352 indiv./km^2, which is much higher than that of Northeast China (approximately 82 indiv./km^2) or China as a whole (135 indiv./km^2). The population density of the Xiliao River basin and the entire Liao River basin is 57 indiv./km^2 and 153 indiv./km^2, respectively (Table 1.). For reference, anthropogenic input to pristine rivers could be neglected for the Amazon, Mackenzie, and Siberian rivers, which have population densities less than 5 indiv./km^2 (Moon et al., 2009). Generally, the plain in the area along the Liao River main stream is covered by cultivated land near cities. Therefore, anthropogenic inputs to rivers of the study area were taken into account using the following calculation.

To estimate the composition of the anthropogenic end-member, we referred to the sewage water collected at Xinmin City (Fig. 1) and Shangzhi City (Liu et al., 2013). Sewage water from the Xinmin City is characterized by high NO_3^- and Na^+ concentrations, with a NO_3/Na molar ratio close to 0.4, whereas that of the Shangzhi is approximately 0, the same as that reported by (Roy et al., 1999). As for the other elements, the Ca, Mg, K, HCO_3, Cl, and Sr to Na ratios and the $^{87}Sr/^{86}Sr$ ratio in the Xinmin and Shangzhi sewage water are 0.68 and 0.52, 0.34 and 0.15, 0.07 and 0.23, 2.38 and 1.38, 1.03 and 0.80, 0.002 and 0.001, and 0.7098 and 0.7087, respectively (Table 2). For the agricultural end-member, we referred to the estimation of Roy et al. (1999) for the Seine River and Chetelat et al. (2008) for the Yangtze River (Changjiang), assuming that only Na, Cl, K and NO_3 are affected by agricultural activities, such as fertilization and/or sewage irrigation. According to regional differences, anthropogenic input to the Dongliao River (sample 11), the Liao River main stream (samples 2 and 4), the Raoyang River (sample 17), the Daling River (sample 18, 19 and 20) and the Hun-Tai River (sample 25) were calculated separately. For details, see Table 4.

5.1.3. Weathering components

5.1.3.1. Evaporites dissolution. The sources of evaporites are not unique and globally vary from a halite end-member to a gypsum end-member; these variable sources are characterized by different SO_4/Na ratios. Furthermore, anthropogenic inputs make estimating the chemical ratios of the evaporite end-members more challenging. The geological map shows that, except for a gypsum-salt layer in the Quaternary deposits, which was considered to be made of gypsum and halite, there is no significant distribution of evaporites in the Liao River basin (Fig. 2). Thus, carbonate + gypsum were considered to be the carbonate end-member, and the evaporite end-member was considered to be only halite (Millot et al., 2003). The element ratios of Cl/Na and Sr/Na were assigned to be 1 and 0.003 for the evaporite (halite) end-member (Vengosh et al., 1995; Krishnaswami and Singh, 1998; Gaillardet et al., 1999, 2003; Millot et al., 2003; Moon et al., 2009). Dissolved K, Mg and HCO_3^- were assumed to be not affected by the dissolution of evaporites. For the $^{87}Sr/^{86}Sr$ ratios, a range of 0.708 ± 0.001 was assigned (Gaillardet et al., 1997; Moon et al., 2009).

5.1.3.2. Silicate weathering. For the inversion calculation, we referred to previous studies (Gaillardet et al., 1999; Han and Liu, 2004; Yang et al., 2004; Wu et al., 2005; Moon et al., 2009), assuming that the silicate chemical ratios of HCO_3/Na, Ca/Na, Mg/Na, K/Na and Sr/Na are 2, 0.35, 0.24, 0.17 and 0.003, respectively.

The $^{87}Sr/^{86}Sr$ ratios of Cenozoic basalts, granite and rocks beneath the Quaternary deposits in northeastern China were reported to be 0.7039–0.7051 (Liu et al., 1995), 0.7047–0.7584 (Yang et al., 2004, 2006), and 0.7046–0.7096 (Wu et al., 2001),

respectively. In the following calculation, the isotope ratio of $^{87}Sr/^{86}Sr$ for the silicate end-member was assigned to be 0.73 ± 0.02 as the a priori silicate end-member for the inversion calculation.

5.1.3.3. Carbonate weathering. Carbonate rocks are distributed separately at the upper reaches of the Xiliao River, Laoha River and Taizi River, the middle reaches of the Daling River, and the drainage area of the Zhaosutai River According (Fig. 2) to the geological map (Fig. 2). As discussed in Section 5.1.3.1, the carbonate end-member in this study is considered the sum of carbonate and gypsum. For the carbonate end-member, element/isotopic ratios of HCO_3/Na, Mg/Na, Ca/Na, Sr/Na and $^{87}Sr/^{86}Sr$ were assigned to be 100, 25, 70, 0.075, and 0.708 according to other studies (Millot et al., 2003; Chetelat et al., 2008; Moon et al., 2009).

5.1.3.4. Sulphide oxidation. Based on the major elements, estimation of the fraction of SO_4 coming from pyrite is a challenge; this value can overestimate or underestimate the weathering fluxes originating from sulfuric acid dissolution. Many studies have shown that the oxidation of sulphide is an important consideration in Chinese Rivers (Han and Liu, 2004; Xu and Liu, 2007; Li et al., 2008, 2011). In this study, most water samples have a SO_4/Ca molar ratio less than 1 (0.3–1.0). SO_4 has a significant positive correlation with Cl ($r^2 = 0.626$, $p < 0.01$) (Table 3), which suggests that they may have similar sources: either atmospheric input or human pollution. Additionally, the positive correlation between SO_4 and Ca is significant ($r^2 = 0.736$, $p < 0.01$), indicating that they both originate from the dissolution of gypsum. Furthermore, the $\delta^{34}S$ values of river water confirms that the SO_4^{2-} is mainly due to the dissolution of gypsum, atmospheric input or human pollution (Tian et al., 2012), and the relationship between the $\delta^{18}O$ of water and that of SO_4 also reveals that only two water samples have the SO_4 derived from sulphide oxidation (unpublished data). Thus, in the following inversion calculation, the sulphide end-member was not taken into account.

5.2. Inversion calculation

5.2.1. The inversion model

In the calculation, an inversion model was used to quantify the relative contributions of the different sources to the dissolved load of the rivers. This method was originally developed in the 1980s for the chemical differentiation of the Earth (Allègre and Lewin, 1989) and was later applied to the calculation of chemical weathering mass budgets (Négrel et al., 1993; Gaillardet et al., 1997, 1999, 2003; Millot et al., 2003; Wu et al., 2005; Chetelat et al., 2008; Moon et al., 2009). The calculation was based on a set of mass budget equations of Na-normalized molar ratios:

$$\left(\frac{X}{\mathrm{Na}}\right)_{river} = \sum_i \left(\frac{X}{\mathrm{Na}}\right)_i \times \alpha_i(\mathrm{Na}); \quad (1)$$

$$\sum_i \alpha_i(\mathrm{Na}) = 1; \quad (2)$$

$$\left(\frac{^{87}\mathrm{Sr}}{^{86}\mathrm{Sr}}\right)_{river} \times \left(\frac{\mathrm{Sr}}{\mathrm{Na}}\right)_{river} = \sum_i \left(\frac{^{87}\mathrm{Sr}}{^{86}\mathrm{Sr}}\right)_i \times \left(\frac{\mathrm{Sr}}{\mathrm{Na}}\right)_i \times \alpha_i(\mathrm{Na}); \quad (3)$$

where *X* stands for Cl, HCO_3, Ca, Mg, K and Sr. In some studies, K was excluded due the possible involvement of vegetation and bacterial activity in the geochemical cycles, which may lead to non-conservative behavior during weathering (Berner and Berner, 1987; Wu et al., 2005). However, to constrain the anthropogenic (agricultural/urban) end-member, we have taken K into account in our study. The subscripts *i* and *river* indicate the *i*th reservoir and river water, respectively. The α_i (Na) is the proportion of sodium (Na) in the river water contributed by the *i*th reservoir. In this study, the 5 reservoirs are considered (n = 5): the atmosphere, anthropogenic input (agricultural/urban), and the three weathering components (evaporites, silicate and carbonate). The normalization to Na is because the sources of Na in river water are clear and are not affected by nutrient cycling (Millot et al., 2003).

In such an approach, there are no data unknowns for the calculation. All variables are parameters for which we, more or less, have information (error bars). The only reasonably well-known parameters are the river parameters, and the least known parameters are the mixing proportions. Starting with an a priori set of compositions for each reservoir, the equations are solved using a least square iterative algorithm by successively iterating the a posteriori values that best fit the whole set of model equations. The contributions of various sources to the dissolved load in the river water and the best values for the elemental ratios of the end-members are calculated simultaneously (Négrel et al., 1993).

5.2.2. Chemical mass balance

Assuming that the dissolved Cl and K are not released by carbonate weathering and HCO_3, Ca, Mg are not affected by anthropogenic inputs, we can write the mass balance equations for each element and the $^{87}Sr/^{86}Sr$ isotopic ratios as follows:

$$[\mathrm{Cl}]_{riv} = [\mathrm{Cl}]_{atm} + [\mathrm{Cl}]_{anth} + [\mathrm{Cl}]_{eva} \quad (4)$$

$$[\mathrm{Ca}]_{riv} = [\mathrm{Ca}]_{atm} + [\mathrm{Ca}]_{sil} + [\mathrm{Ca}]_{carb} \quad (5)$$

$$[\mathrm{Mg}]_{riv} = [\mathrm{Mg}]_{atm} + [\mathrm{Mg}]_{sil} + [\mathrm{Mg}]_{carb} \quad (6)$$

$$[\mathrm{Na}]_{riv} = [\mathrm{Na}]_{atm} + [\mathrm{Na}]_{anth} + [\mathrm{Na}]_{eva} + [\mathrm{Na}]_{sil} + [\mathrm{Na}]_{carb} \quad (7)$$

$$[\mathrm{K}]_{riv} = [\mathrm{K}]_{atm} + [\mathrm{K}]_{anth} + [\mathrm{K}]_{sil} \quad (8)$$

$$[\mathrm{HCO_3}]_{riv} = [\mathrm{HCO_3}]_{sil} + [\mathrm{HCO_3}]_{carb} \quad (9)$$

$$[\mathrm{Sr}]_{riv} = [\mathrm{Sr}]_{atm} + [\mathrm{Sr}]_{eva} + [\mathrm{Sr}]_{sil} + [\mathrm{Sr}]_{carb} \quad (10)$$

$$[^{87}\mathrm{Sr}/^{87}\mathrm{Sr}]_{riv} = \sum \alpha_i (^{87}\mathrm{Sr}/^{87}\mathrm{Sr})_i \quad (11)$$

where the subscript *riv* stands for river, *atm* for atmospheric, *anth* for anthropogenic, *eva* for evaporites, *sil* for silicate and *carb* for car-

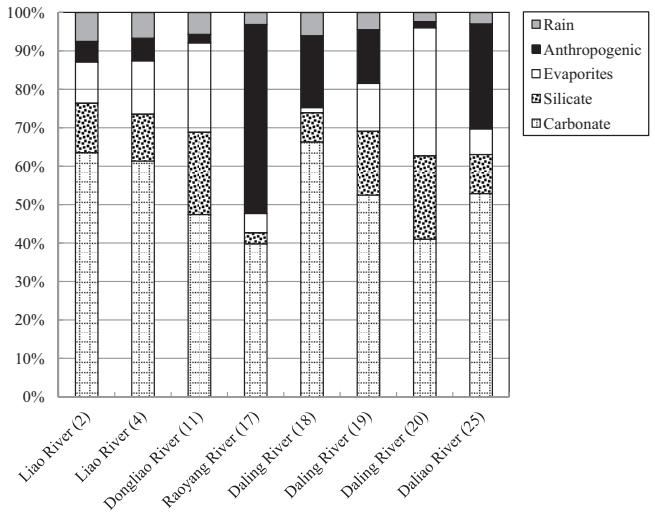

Fig. 6. Calculated contributions of the different reservoirs to the cationic TDS (mg/L) from the inversion method for the Liao River main stream and some tributaries. Numbers in the brackets are samples used in the calculation for each river.

Table 5
Cationic TDS (mg/L) derived from the atmospheric and anthropogenic inputs, the weathering of evaporites, silicate and carbonate calculated by the inversion model for the Liao River and some tributaries.

Rivers	Samples	Atmospheric	Anthropogenic	Evaporites	Silicate	Carbonate
Liao River	2	4.49 ± 0.35	3.20 ± 1.92	6.44 ± 1.11	7.69 ± 2.40	38.1 ± 8.7
Liao River	4	4.58 ± 0.35	4.06 ± 2.74	9.55 ± 1.86	8.36 ± 3.48	42.2 ± 9.1
Dongliao River	11	5.49 ± 0.42	2.19 ± 2.02	22.6 ± 1.80	20.8 ± 4.65	46.1 ± 13
Raoyang River	17	4.54 ± 0.35	71.4 ± 6.50	7.32 ± 6.46	4.16 ± 3.10	57.9 ± 12
Daling River	18	4.45 ± 0.34	13.8 ± 3.78	1.00 ± 3.38	5.62 ± 4.14	49.0 ± 9.2
Daling River	19	4.57 ± 0.35	14.3 ± 6.86	12.7 ± 5.95	17.0 ± 7.93	53.7 ± 12
Daling River	20	4.54 ± 0.35	3.13 ± 9.04	64.4 ± 5.92	42.0 ± 6.62	79.3 ± 21
Daliao River	25	2.37 ± 0.18	22.0 ± 4.81	5.39 ± 4.21	8.19 ± 5.57	42.7 ± 10

The incertitudes are estimated from the inverse model.

bonate. For Eq. (11), α is the proportion of Sr derived from the i^{th} reservoir. As discussed in Section 5.2.1, instead of the absolute concentrations, the Na-normalized mass balance equations were used in the calculation.

5.2.3. Inversion results

The calculated contributions of the different reservoirs to the cationic TDS (mg/L) for the Liao River and some tributaries are illustrated in Fig. 6, and the values are listed in Table 5. Generally, TDS (mg/L) of the rivers are dominated by carbonate (+gypsum) weathering, ranging from 40% (Raoyang River) to 66% (Daling River, sample 18) with an average of 53% for the rivers in this analysis. The water in the main stream of the Liao River is mainly derived from the two biggest head streams: the Xiliao River (annual discharge 26.7×10^8 m^3/yr), draining carbonate areas in the upper reaches, and the Dongliao River (annual discharge 8.36×10^8 m^3/yr), which has a carbonate (+gypsum) contribution of 47% to the cationic TDS. Therefore, for the Liao River main stream, carbonate (+gypsum) weathering accounts for more than 60% of the cationic TDS (samples 2 and 4). The Daliao River (Hun-Tai River) and the Daling River have carbonate (+gypsum) proportions of 53% (sample 25) and 40–66% (samples 18–20), respectively, reflecting that the river water of these two rivers is affected by the weathering of the carbonate rocks found in the upper reaches of the Taizi River (Liu, 2007) and the middle reaches of the Daling River. Travelling upstream (sample 2) to downstream (sample 4) along the Liao River main stream, contributions from each reservoir are relatively constant due to a lack of large tributaries. For the Daling River, the contribution of carbonate (+gypsum) decreases from upstream to downstream.

Overall, the contribution of silicate weathering is variable, ranging from 3% (Raoyang River, sample 17) to 22% (Daling River, sample 20) with an average of 13% for the rivers involved in this analysis. These levels are governed by the distributions of silicate rocks in the basin. For the main stream of the Liao River, the upper reaches of the Dongliao River, the Daling River, and the Daliao River (Hun-Tai River), these levels are approximately 12–13%, approximately 21%, 8–22% and 10%, respectively. The contribution of evaporites to the cationic load ranges from 1% to 33% and accounts for less than 14% of the TDS of the rivers studied, except for the Donliao River and the lower reaches of the Daling River.

Atmospheric inputs are, in general, minor contributors to the cation levels, ranging from 2% to 7%, with an average of 5%.

Contribution of human activities (agricultural, industrial or domestic input) to the cationic TDS in the Liao River and its tributaries is variable, ranging from 2% in the Daling River (sample 20) to 49% in the Raoyang River (sample 17). For the main stream of the Liao River, anthropogenic inputs are relatively small (approximately 5–6%) because of the sparse population density in the upper reaches. As previously discussed, cities, population and agriculture are mainly distributed in the plain in the center of the Liao River basin. From Fig. 6, we can see that the Raoyang River, which flows through the plains, appears to be affected by human activities due to the high population density (Table 2). In the upper reaches, the Daling River is highly affected by domestic and industrial pollutants, and approximately 19% of the cationic TDS is from anthropogenic inputs. From upstream to downstream, the contribution of anthropogenic input to the cationic TDS became lower and lower as a result of a stronger dilution effect and the increasing effects of other end-members. Anthropogenic input to the Daliao River (Hun-Tai River) was approximately 27%, indicating that the river is also heavily impacted by human activities.

5.3. Chemical weathering rates and associate CO_2 consumption

The rate of cationic weathering rates (in t/km^2/yr) represented as a weathering index was calculated using Eqs. (12) and (13). According to Millot et al. (2003) and Chetelat et al. (2008), assuming that all of the aqueous silica composition was derived from silicate weathering, the silicate-derived TDS_{sil} was calculated as the $Cation_{sil}$ plus the silicate-yield HCO_3 and SiO_2 in the river water (Eq. (14)). Similarly, carbonate (+gypsum) derived TDS_{carb} was calculated using Eq. (15):

$$Cation_{sil} = 23 * [Na]_{sil} + 39 * [K]_{sil} + 40 * [Ca]_{sil} + 24 * [Mg]_{sil} \quad (12)$$

$$Cation_{carb} = 40 * [Ca]_{carb} + 24 * [Mg]_{carb} \quad (13)$$

$$TDS_{sil} = 23 * [Na]_{sil} + 39 * [K]_{sil} + 40 * [Ca]_{sil} + 24 * [Mg]_{sil} + 60 * [SiO_2]_{riv} + 61 * [HCO_3]_{sil} \quad (14)$$

$$TDS_{carb} = 40 * [Ca]_{carb} + 39 * [Mg]_{carb} + 61 * 1/2[HCO_3]_{carb} \quad (15)$$

CO_2 consumption from silicate weathering ($CO_{2\text{-}sil}$) is calculated according to the charge balance between the silicate-derived alkalinity and the silicate-derived cations and is independent of the aqueous silica concentration:

$$CO_{2-sil} = 61^*[HCO_3]_{sil} \quad (16)$$

The consumption of CO_2 by carbonate weathering is calculated as follows:

$$[CO_2]_{carb} = 61^*1/2[HCO_3]_{carb} \quad (17)$$

Acids that are derived directly from the atmosphere (i.e., CO_2) or produced by the remineralization of organic matter in soil contribute to the dissolution of rocks (Lerman et al., 2007). Several studies have shown that H_2SO_4 plays an important role in rock weathering (Xu and Liu, 2007; Chetelat et al., 2008; Li et al., 2008, 2011; Han et al., 2010). Sulfuric acid can be produced naturally through the oxidation of pyrite in sediments and anthropogenic emissions of SO_2 from coal combustion. Reactions of dissolved CO_2 and H_2SO_4 with carbonate and silicate minerals are described according to Lerman et al. (2007), Xu and Liu (2007) and Chetelat et al. (2008) as follows:

Weathering of carbonate minerals by H_2CO_3 and H_2SO_4:

$$Ca_xMg_{1-x}CO_3 + H_2CO_3 \rightarrow xCa^{2+} + (1-x)Mg^{2+} + 2HCO_3^- \quad (18)$$

$$2Ca_xMg_{1-x}CO_3 + H_2SO_4 \rightarrow 2xCa^{2+} + 2(1-x)Mg^{2+} + 2HCO_3^- + SO_4^{2-} \quad (19)$$

$$3Ca_xMg_{1-x}CO_3 + H_2SO_4 + H_2CO_3 \rightarrow 3xCa^{2+} + 3(1-x)Mg^{2+} + 4HCO_3^- + SO_4^{2-} \quad (20)$$

Weathering of silicate minerals by H_2CO_3 and H_2SO_4 acids:

For divalent-cation silicates:

$$CaAl_2Si_2O_8 + 2CO_2 + 4H_2O \rightarrow Ca^{2+} + 2HCO_3^- + 2SiO_2 + 2Al(OH)_3 \quad (21)$$

$$CaAl_2Si_2O_8 + H_2SO_4 \rightarrow Ca^{2+} + SO_4^{2-} + 2SiO_2 + 2AlOOH \quad (22)$$

For monovalent-cation silicates:

$$NaAlSi_3O_8 + CO_2 + 2H_2O + \rightarrow Na^+ + HCO_3^- + 3SiO_2 + Al(OH)_3 \quad (23)$$

$$NaAlSi_3O_8 + H_2SO_4 \rightarrow Na^+ + SO_4^{2-} + 6SiO_2 + AlOOH \quad (24)$$

Evidence of the involvement of protons originating from H_2SO_4 is given by Fig. 7. From Eqs. (17), (21) and (23), it can be concluded that if there is no sulfuric acid involved in the weathering process, the equivalent ratio of the DIC and the sum of the cations released by silicate and carbonate (+gypsum) should be 1:1. Our data deviate from the 1:1 line (Fig. 7), indicating that weathering by H_2SO_4 is important and increases the chemical weathering of rocks. However, due to the low reactivity of silicates compared to carbonates, the interaction of the sulphide-derived protons with silicate minerals is less probable (Millot et al., 2003). Because carbonate weathering dominates the TDS of the Liao River Basin, the involvement of sulfuric acid in silicate weathering is not considered in this study.

Based on Eqs. (18) and (19), carbonate weathering by both carbonic and sulfuric acids is shown by Eq. (25):

$$3Ca_xMg_{1-x}CO_3 + H_2SO_4 + H_2CO_3 \rightarrow 3xCa^{2+} + 3(1-x)Mg^{2+} + 4HCO_3^- + SO_4^{2-} \quad (25)$$

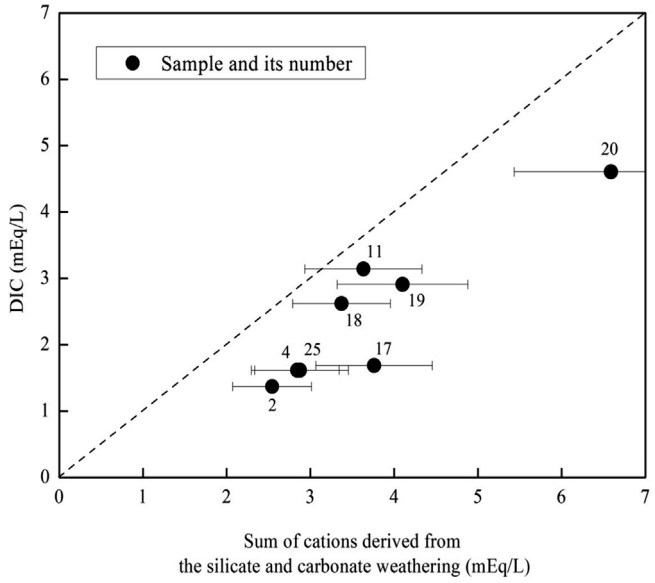

Fig. 7. DIC as a function of the sum of the cations derived from carbonate (+gypsum) and silicate weathering.

Thus, the carbonate yield TDS_{carb} for the involvement of both carbonic acid and sulfuric acid in the weathering of carbonate rocks and CO_2 related consumption can be calculated as Eqs. (26) and (27), respectively.

$$TDS_{carb} = 40 * [Ca]_{carb} + 39 * [Mg]_{carb} + 61^*3/4[HCO_3]_{carb} \quad (26)$$

$$[CO_2]_{carb} = 61 * 1/4[HCO_3]_{carb} \quad (27)$$

The chemical weathering rates of different types of rocks and the associated CO_2 consumption rates were estimated using the last samples for each river basin: sample 20 for the Daling River, sample 25 for the Hun-Tai River (Daliao River), sample 17 for the Raoyang River, sample 11 for the Dongliao River, and samples 2 and 4 for the Liao River main stream. For the Xiliao River, we cannot reach a result for the inversion calculation by using the a priori end-member composition designed for the other rivers, so the chemical weathering rates of the Xiliao River basin were not estimated in this study. As discussed above, sample 5 (the Liao River downstream) may have been polluted by seawater/sewage water; thus, sample 4 was used in the calculation.

The results (Table 6) shows that the Hun-Tai River basin (the Daliao River) and the Daling River basin have the highest carbonate (+gypsum) and silicate weathering rates. In contrast, the Raoyang River basin has the lowest weathering rates for all types of rocks, with weathering rates less than 1. The $cation_{sil}$ weathering rates are highly variable for the sub-basins, ranging from 0.03 ± 0.02 (Raoyang River) to 3.17 ± 0.50 t/km^2/yr (Daling River). However, the estimated $cation_{sil}$ weathering rates for the Liao River main stream are relatively constant with an upstream (sample 2) value of 0.20 ± 0.05 and a downstream (sample 4) value of 0.26 ± 0.08 t/km^2/yr. Similarly, the $cation_{carb}$ weathering rate varies across the sub-basins from 0.39 ± 0.08 (Raoyang River) to 10.3 ± 2.46 t/km^2/yr (Hun-Tai River), whereas it is relatively constant for the Liao River mainstream. The upstream (sample 2) and downstream (sample 4) values for the $cation_{carb}$ weathering rate are 0.97 ± 0.22 and 1.30 ± 0.28 t/km^2/yr, respectively.

As was the case with the rock weathering rates, the Daling River and the Hun-Tai River have the highest CO_2 consumption rates by silicate weathering and carbonate weathering, respectively. The Raoyang River has the lowest CO_2 consumption rates for all types of rock weathering. The estimated CO_2 consumption rates of the Liao River main stream are constant from upstream (6.66×10^3 mol/km^2/yr at sample 2) to downstream (10.1×10^3 mol/km^2/yr at sample 4). These rates for the Daling River (138×10^3 mol/km^2/yr) and Dongliao River (100×10^3 mol/km^2/yr) are much higher than those for the Liao main stream (10.1×10^3 mol/km^2/yr at sample 4) and Raoyang River (0.95×10^3 mol/km^2/yr at sample 4) by one or two orders of magnitude.

It should be mentioned that similar to most previous related studies of large rivers in the world, the above estimations of the weathering and CO_2 consumption rates are based on the data from one field campaign, which may bring uncertainty when used to represent the situation over a year or longer. The uncertainties presented in this study did not consider temporal variations of the solutes and river water discharge. Another source of uncertainties is the effects of natural and artificial reservoirs on chemical weathering. This is a priori the case for the Liao and its tributaries for which aforementioned, there has been a noticeable increase in dam (and other water conservation project) built in Liao River basin in recent years, which may impact the water discharge, sediment load (Liu et al., 2007), water chemistry (Wang et al., 2010), and thus the chemical weathering and CO_2 consumption rates. However, because of the lack of historic data, it is not possible to specify this type of human disturbance.

Table 6
Chemical weathering and CO_2 consumption rates for the Liao River Basin, NE China.

Basins	No. of sample used	Discharge (10^8 m^3/yr)	Drainage area (km^2)	Silicates				Carbonates					Evaporites	Total rock weathering TDS (t/km^2/yr)
				$Cation_{sil}$[a] (t/km^2/yr)	TDS_{sil}[b] (t/km^2/yr)	$(Ca + Mg)_{sil}$[c] (10^9 mol/yr)	CO_2[d] cons. (10^3 mol/km^2/yr^1)	$Cation_{carb}$[e] (t/km^2/yr)	By only carbonic acids		By both sulfuric and carbonic acids		TDS_{eva}[f] (t/km^2/yr)	
									TDS_{carb}[b] (t/km^2/yr)	CO_2 cons.[d] (10^3 mol/km^2/yr^1)	TDS_{carb}[b] (t/km^2/yr)	CO_2 cons.[d] (10^3 mol/km^2/yr^1)		
Liao River	2	30.8	120,764	0.20 ± 0.05	0.31 ± 0.05	0.28 ± 0.13	6.66 ± 5.35	0.97 ± 0.22	1.83 ± 0.34	14.1 ± 4.17	2.26 ± 0.44	7.03 ± 2.08	0.42 ± 0.05	2.96 ± 0.48
Liao River	4	59.1	191,683	0.26 ± 0.08	0.28 ± 0.08	0.58 ± 0.32	10.1 ± 8.78	1.30 ± 0.28	2.51 ± 0.45	19.9 ± 5.65	3.12 ± 0.59	9.94 ± 2.83	0.75 ± 0.11	4.16 ± 0.71
Dongliao River	11	8.36	10,228	1.70 ± 0.34	2.20 ± 0.34	0.20 ± 0.08	100 ± 42.1	3.77 ± 1.04	8.54 ± 1.85	78.3 ± 25.1	10.9 ± 2.52	39.1 ± 12.5	4.70 ± 0.27	21.6 ± 3.19
Raoyang River	17	0.67	9950	0.03 ± 0.02	0.04 ± 0.02	0.0033 ± 0.003	0.95 ± 1.31	0.39 ± 0.08	0.70 ± 0.12	5.15 ± 1.48	0.86 ± 0.16	2.57 ± 0.74	0.12 ± 0.08	0.92 ± 0.16
Daling River	20	17.5	23,263	3.17 ± 0.50	3.84 ± 0.50	0.88 ± 0.28	138 ± 51.1	5.98 ± 1.58	12.4 ± 2.65	105 ± 34.9	15.6 ± 3.56	52.4 ± 17.4	12.4 ± 1.08	36.9 ± 4.26
Hun-Tai River	25	66.2	27,327	1.98 ± 0.99	2.80 ± 0.99	0.64 ± 0.50	69.0 ± 86.6	10.3 ± 2.46	20.1 ± 3.96	161 ± 50.8	25.0 ± 5.26	80.4 ± 25.4	3.32 ± 1.88	30.5 ± 6.93
Other riversi of China														
Huanghe r (Yellow Rive[g]	–	410	752,443	2.13	3.46	19.0	82.4	–	–	–	4.65	39.9	6.65	14.8
Chanjiang (Yangtze River)[h]	CJ-36	8650	1,705,000	2.40	2.35	43.0	112	14.0	–	–	36.4	379	4.11	42.8
Xijiang River[i]	49	2300	352,000	3.26	7.45	13.9	154	30.0	–	–	78.5	807	0.20	86.1

[a] $Cation_{sil:}$ the sum of cation (Na + K + Ca + Mg) concentrations derived from silicate weathering. The incertitudes are estimated from the inverse model.
[b] See text for TDS_{sil} and TDS_{carb}.
[c] $(Ca + Mg)_{sil}$: the sum of Ca + Mg derived from silicate weathering.
[d] CO_2 cons.: the CO_2 consumption rates based on the cation contribution.
[e] $Cation_{Carb}$: the sum of cation (Ca + Mg) concentrations derived from carbonate weathering.
[f] TDS_{eva} values are calculated based on Na and Ca + Mg estimated from the mass budget and their stoichiometric equivalent of Cl and SO_4, respectively.
[g] Gaillardet et al. (1999).
[h] Chetelat et al. (2008).
[i] Xu and Liu (2010).

5.4. Comparison with global rivers

Except for the Raoyang River (0.03 ± 0.02 t/km^2/yr) and the main stream of the Liao River (0.26 ± 0.08 t/km^2/yr), the $cation_{sil}$ weathering rates of the rivers from the study area are on the same order of magnitude as those of other large river basins in China. Compared with the rivers draining regions with temperate climates, the flux of $Cation_{sil}$ in the Liao River main stream (0.26 ± 0.08 t/km^2/yr.) are ranked the following order: The Liao River < Amur River [0.67 t/km^2/yr, (Moon et al., 2009)] < Nenjiang River [0.86 t/km^2/yr, (Liu et al., 2013)] < Songhuajiang [1.44 t/km^2/yr, (Liu et al., 2013)] < 2nd Songhua River [2.91 t/km^2/yr, (Liu et al., 2013)], and is lower than those of the Huanghe [2.13 t/km^2/yr, (Gaillardet et al., 1999)], Changjiang [2.40 t/km^2/yr, (Chetelat et al., 2008)], the Xijiang [3.26 t/km^2/yr, (Xu and Liu, 2007)], and Amazon rivers that drain orogenic regions [5.34 t/km^2/yr, (Moon et al., 2009)]. The $cation_{sil}$ weathering rates of the Daling River (3.17 ± 0.50 t/km^2/yr) and Hun-Tai River (1.98 t/km^2/yr) are higher than those of most of the world's large rivers. The CO_2 consumption rate for the Liao River main stream (10.1×10^3 mol/km^2/yr) is at the lower end of the spectrum for the world's large rivers and is on the same order of magnitude observed for the Seine River [13×10^3 mol/km^2/yr, (Gaillardet et al., 1999)]. The highest CO_2 consumption rate in the study area (the Daling River, 138×10^3 mol/km^2/yr) is higher than those of most of the world's large rivers and is close to that of the Brahmaputra [(150×10^3 mol/km^2/yr), (Gaillardet et al., 1999)].

For the $cation_{carb}$ weathering rate, the Liao River main stream (1.30 ± 0.28 t/km^2/yr, at sample 4) is close to that of the Nenjiang River [1.22 t/km^2/yr, (Liu et al., 2013) and the Songhuajiang River [1.89 t/km^2/yr, (Liu et al., 2013)]; it is also much lower than that of the Seine River [18 t/km^2/yr, (Roy et al., 1999)]. The rate of $Cation_{carb}$ of the Hun-Tai River (10.3 t/km^2/yr) is on the same order of magnitude as that of the Changjiang [14.0 t/km^2/yr, (Chetelat et al., 2008)]. For the TDS_{carb} and CO_2 consumption rates by carbonate (+gypsum) weathering, we used the results calculated for the case in which carbonate was attacked by both carbonic acids and sulfuric acids in the discussion, which is closer to the natural situation. TDS yield by carbonate (+gypsum) weathering of the Liao River main stream (3.12 ± 0.59 t/km^2/yr) is relatively low compared to global rivers and is close to that of the Yellow River [4.7 t/km^2/yr, (Gaillardet et al., 1999)] and the Amur River (3.9 t/km^2/yr). The highest value of TDS_{carb} was observed at the Hun-Tai River (25.0 t/km^2/yr), which is on the same order of magnitude as that of Changjiang [36.4 t/km^2/yr, (Chetelat et al., 2008)]. The CO_2 consumption rates by carbonate (+gypsum) weathering in the study area are highly variable, ranging from 2.57×10^3 mol/km^2/yr to 80.4×10^3 mol/km^2/yr. The highest value was observed at the Hun-Tai River, which is much lower than that of rivers draining carbonate-rich areas such as Xijiang [807×10^3 mol/km^2/yr, (Xu and Liu, 2007)] and Wujiang [682×10^3 mol/km^2/yr, (Han and Liu, 2004)]. Among the global large rivers, CO_2 consumption rates by carbonate (+gypsum) weathering of the Liao River main stream (9.94×10^3 mol/km^2/yr, at sample 4) is among the lowest and is only higher than that of the Murray Darling River from Australia (5×10^3 mol/km^2/yr) and the Nile from Africa [4×10^3 mol/km^2/yr, (Gaillardet et al., 1999)].

5.5. Controlling factors

Admittedly, many factors control the chemical weathering rates within river basins, and these factors can be broadly classified as lithologic, climatic (temperature, runoff), tectonic, biological and geomorphological (Gislason et al., 2009; Viers et al., 2014). However, these factors do not act independently of one another, and there are many important interlinkages (Goudie and Viles, 2012). It is very difficult to isolate the impact of any one controlling factor on the weathering rates; similarly, the dominant factors are difficult to determine due to the variable control mechanisms that depended on different conditions. Thus, more and better datasets on chemical weathering and the factors that control it are needed.

Among all of the factors controlling chemical weathering rates, lithology is the most important because different types of rocks have different characteristics and different weathering abilities (Viers et al., 2014). For the study area, silicate rocks are mainly distributed at the upper reaches of the Xiliao, Dongliao, and Hun-Tai Rivers as well as most of the Daling River drainage area. Accordingly, the silicate weathering rates are higher in these regions than in others. According to (Liu, 2007), carbonate rocks could be observed at the upper reaches of the Laoha and Taizi Rivers, the middle reaches of the Daling River, and the drainage area of the Zhaosutai River. Therefore, leaving out other controlling factors, the Daling River, the Hun-Tai River and the Dongliao River have relatively higher $cation_{carb}$ weathering rates than the Liao main stream, and the rate for the Raoyang River is the lowest.

Climate also acts as a major factor controlling chemical weathering (Gislason et al., 2009; Eiriksdottir et al., 2011; Liu et al., 2013). A linear correlation between the cationic weathering rates of carbonate and runoff (in a log–log space) was observed for the Liao River Basin (and 6 other large rivers with available data) (Fig. 8a), indicating that the dominant parameter controlling the carbonate weathering rate of the Liao River basin is runoff. Simi-

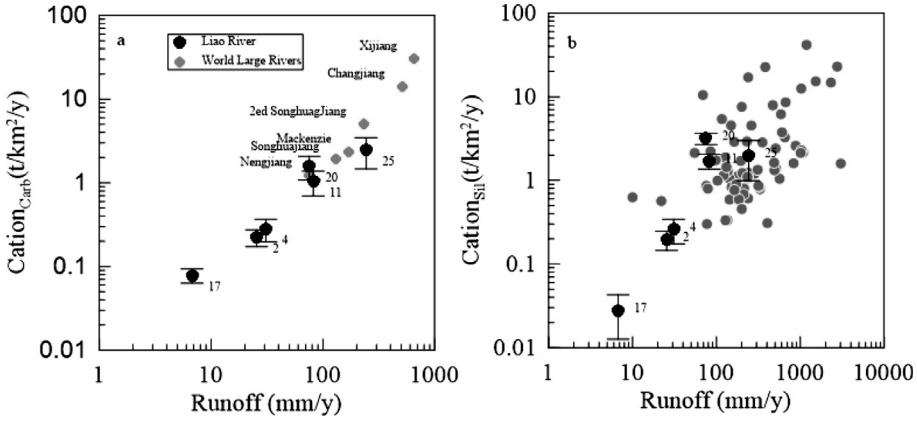

Fig. 8. The log-log relationship between the cationic chemical weathering rates and runoff for (a) carbonate (+gypsum) and (b) silicate (sample numbers used in the calculation are listed beside the symbol *Data sources:* Gaillardet et al. (1999) (world large rivers), Chetelat et al. (2010) (Changjiang), Xu and Liu (2010) (Xijiang), Millot et al. (2003) (Mackenzie) and Liu et al. (2013) (Songhuajiang, 2nd Songhuajian and Nengjiang).

larly, with the exception of the Dongliao (sample 11) and Daling Rivers (sample 20), $cation_{sil}$ of most studied rivers also show a liner relationship with runoff (Fig. 8b). This result reveals that the dominating factor controlling the silicate weathering rate in the Liao River basin is runoff. Although there is not a linear relationship, the $cation_{sil}$ of all of the plotted rivers shows a trend toward increasing with runoff (Fig. 8b), indicating the influence of runoff on silicate weathering. This result is similar to many previous studies (White and Blum, 1995; Gaillardet et al., 1999; Millot et al., 2003; Wu et al., 2005; Chetelat et al., 2008) and was highlighted by Shin et al. (2011) in that there is an expected seasonal difference of chemical weathering.

Human activities affect chemical weathering by causing acidic precipitation through the release of SO_2, which could be involved in the chemical weathering process (Karim and Veizer, 2000; Han and Liu, 2004; Li et al., 2008; Xu and Liu, 2010; Ding et al., 2013). Anthropogenic influence could change the river water chemistry by discharging wastewater, fertilization, deforestation and forest management (Raymond et al., 2008). The magnitude of the carbonate (+gypsum)-yield TDS_{carb} was on the same order of magnitude, regardless of whether carbonate rocks are attacked only by carbonic acids or by both carbonic and sulfuric acid. This result indicated that the effect of sulfuric acids on the weathering of carbonate (+gypsum) (TDS) in the study area was unlike other basins in China (Li et al., 2008; Han et al., 2010; Xu and Liu, 2010). However, human activities very obviously affect the weathering rates. Notably, the Raoyang River, seriously affected by human activities, has the proportion of anthropogenic cation input reaching 49% and the lowest chemical rates. It is obvious that in addition to the less distribution of silicate and/or carbonate rock and lower runoff within the basin, human activities must be considered as another important parameters in river water analyses.

6. Conclusion

The chemical compositions of the major ions in the Liao River water show that the weathering of carbonate (+gypsum) and anthropogenic inputs provide the majority of the solutes in the river water. For all of the river water samples, Ca^{2+} is the most abundant cation, accounting for 39% of the total cations (TZ^+), and is followed by Na^+ and Mg^{2+} at 34% and 25% of the total cations, respectively. HCO_3^- is the dominant anion, accounting for 48% of the total anion concentration (TZ^-), followed by Cl^- and SO_4^{2-}, at 26% and 24%, respectively.

The results of the inverse model showed that the dissolved cationic loads in the studied rivers originated mostly from carbonate (+gypsum) weathering (53%) and anthropogenic inputs (16%). The Raoyang River, which drains the lower Liao River Plain, is seriously affected by human activities with the proportion of anthropogenic cation input as high as 49%. The Daling River basin has the highest silicate weathering rates (TDS_{sil}, 3.84 t/km^2/yr) and the Hun-Tai River basin (Daliao River) has the highest carbonate (+gypsum) weathering rates (TDS_{carb}, 25.0 t/km^2/yr). Chemical weathering in the study area is controlled by lithology and runoff and is affected by human activity. However, lack of temporal and historic data brought uncertainties to our estimation of chemical weathering rates in Liao River system, both short-term and long-term studies are needed to get a better understanding of chemical weathering rate and controlling factors.

Acknowledgments

This study is financially supported by National Natural Science Foundation of China (Grant Nos. 41130536, 41203090, 41372376), the water project of the MEP (2012ZX07503003001), and by The State Key Laboratory of Environmental Geochemistry (SKLEG2015407). The authors thank Prof. Benjamin Chetelat (now at Tianjin University, China) for help with the inverse model, and Ms. Yanning Deng (Tianjin Normal University, China), Zhuojun Zhang and Mr. Lihua Zhang (Institute of Geochemistry, CAS) for assistance in sampling. Jin Guan, Yuhong Fan, Rongsheng Huang and Hongwen Ling (Institute of Geochemistry, CAS) are acknowledged for chemical analyses.

References

Allègre, C.J., Lewin, E., 1989. Chemical structure and history of the Earth: evidence from global non-linear inversion of isotopic data in a three-box model. Earth Planet. Sci. Lett. 96, 61–88.
Berner, E.K., Berner, R.A., 1987. Global Water Cycle: Geochemistry and Environment. Prentice-Hall, New Jersey.
Blum, J.D., Erel, Y., 1997. Rb Sr isotope systematics of a granitic soil chronosequence: the importance of biotite weathering. Geochim. Cosmochim. Acta 61, 3193–3204.
Chai, F., Gao, J., Wang, S., Zhang, Q., Chen, Y., Zhang, X., Zhang, M., 2010. The characteristics of precipitation chemistry and its relationship with atmospheric transport at a background site in Liaoning province (in Chinese). Res. Environ. Sci. 23, 387–393.
Chetelat, B., Liu, C.Q., Zhao, Z., Wang, Q., Li, S., Li, J., Wang, B., 2008. Geochemistry of the dissolved load of the Changjiang Basin rivers: Anthropogenic impacts and chemical weathering. Geochim. Cosmochim. Acta 72, 4254–4277.
Ding, H., Lang, Y.-C., Liu, C.-Q., Liu, T.-Z., 2013. Chemical characteristics and dS^{34}-SO_4^{2-} of acid rain: anthropogenic sulfate deposition and its impacts on CO_2 consumption in the rural karst area of southwest China. Geochem. J. 47, 625–638.
Eiriksdottir, E.S., Gislason, S.R., Oelkers, E.H., 2011. Does runoff or temperature control chemical weathering rates? Appl. Geochem. 26 (Supplement), S346–S349.
Güler, C., Thyne, G., McCray, J., Turner, K., 2002. Evaluation of graphical and multivariate statistical methods for classification of water chemistry data. Hydrogeol. J. 10, 455–474.
Gaillardet, J., Dupré, B., Allègre, C.J., Négrel, P., 1997. Chemical and physical denudation in the Amazon River Basin. Chem. Geol. 142, 141–173.
Gaillardet, J., Dupré, B., Louvat, P., Allègre, C.J., 1999. Global silicate weathering and CO_2 consumption rates deduced from the chemistry of large rivers. Chem. Geol. 159, 3–30.
Gaillardet, J., Millot, R., Dupré, B., 2003. Chemical denudation rates of the western Canadian orogenic belt: the Stikine terrane. Chem. Geol. 201, 257–279.
Gislason, S.R., Oelkers, E.H., Eiriksdottir, E.S., Kardjilov, M.I., Gisladottir, G., Sigfusson, B., Snorrason, A., Elefsen, S., Hardardottir, J., Torssander, P., Oskarsson, N., 2009. Direct evidence of the feedback between climate and weathering. Earth Planet. Sci. Lett. 277, 213–222.
Goudie, A.S., Viles, H.A., 2012. Weathering and the global carbon cycle: geomorphological perspectives. Earth Sci. Rev. 113, 59–71.
Han, G., Liu, C.-Q., 2004. Water geochemistry controlled by carbonate dissolution: a study of the river waters draining karst-dominated terrain, Guizhou Province, China. Chem. Geol. 204, 1–21.
Han, G., Tang, Y., Xu, Z., 2010. Fluvial geochemistry of rivers draining karst terrain in Southwest China. J. Asian Earth Sci. 38, 65–75.
Jin, L., Ogrinc, N., Yesavage, T., Hasenmueller, E.A., Ma, L., Sullivan, P.L., Kaye, J., Duffy, C., Brantley, S.L., 2014. The CO_2 consumption potential during gray shale weathering: insights from the evolution of carbon isotopes in the Susquehanna Shale Hills critical zone observatory. Geochim. Cosmochim. Acta 142, 260–280.
Karim, A., Veizer, J., 2000. Weathering processes in the Indus River Basin: implications from riverine carbon, sulfur, oxygen, and strontium isotopes. Chem. Geol. 170, 153–177.
Krishnaswami, S., Singh, S., 1998. Silicate and carbonate weathering in the drainage basins of the Ganga-Ghaghara-Indus head waters: contributions to major ion and Sr isotope geochemistry. Proc. Indian Acad. Sci. Earth Planet. Sci. 107, 283–291.
Kump, L.R., Brantley, S.L., Arthur, M.A., 2000. Chemical weathering, atmospheric CO_2, and climate. Annu. Rev. Earth Planet. Sci. 28, 611–667.
Lang, Y.-C., Liu, C.-Q., Zhao, Z.-Q., Li, S.-L., Han, G.-L., 2006. Geochemistry of surface and ground water in Guiyang, China: water/rock interaction and pollution in a karst hydrological system. Appl. Geochem. 21, 887–903.
Lerman, A., Wu, L., Mackenzie, F.T., 2007. CO_2 and H_2SO_4 Consumption in Weathering and Material Transport to the Ocean, and their Role in the Global Carbon Balance.
Li, S.-L., Calmels, D., Han, G., Gaillardet, J., Liu, C.-Q., 2008. Sulfuric acid as an agent of carbonate weathering constrained by $\delta^{13}C_{DIC}$: examples from Southwest China. Earth Planet. Sci. Lett. 270, 189–199.
Li, X.-D., Liu, C.-Q., Liu, X.-L., Bao, L.-R., 2011. Identification of dissolved sulfate sources and the role of sulfuric acid in carbonate weathering using dual-isotopic data from the Jialing River, Southwest China. J. Asian Earth Sci. 42, 370–380.
Li, X., Li, X., 1996. Chemical composition in precipitation water in the suburban area of Chifeng City (in Chinese). Inner Mongolia Environ. Prot. 8, 13–15.
Li, Y.L., Liu, K., Li, L., Xu, Z.X., 2012. Relationship of land use/cover on water quality in the Liao River basin, China. Proc. Environ. Sci. 13, 1484–1493.

Liu, B., Liu, C.-Q., Zhang, G., Zhao, Z.-Q., Li, S.-L., Hu, J., Ding, H., Lang, Y.-C., Li, X.-D., 2013. Chemical weathering under mid- to cool temperate and monsoon-controlled climate: a study on water geochemistry of the Songhuajiang River system, northeast China. Appl. Geochem. 31, 265–278.
Liu, C., Wang, Z., Tuo, J., 2007. Analysis on variation of seagoing water and sediment load in main rivers of China (in Chinese). J. Hydraulic Eng. 38, 1444–1452.
Liu, C., Xie, G., Masuda, A., 1995. Geochemistry of cenozoic basalts from eastern China (II): Sr, Nd and Ce isotopic compositions (in Chinese). Geochimica 24, 203–214.
Liu, J., 2007. Some Strategy Researches on Soil and Water Resources Allocation, Ecological and Environmental Protection and Sustainable Development in the Northeast China: Comprehensive Volume: Volum Natural History (in Chinese). Science Press, Beijing.
Liu, Z., 2008. The Chemical Character of Acid Precipitation in Liaozhong Area (in Chinese). Shandong Normal University, Ji'nan, p. 58.
Meybeck, M., 1983. Atmospheric inputs and river transport of dissolved substances. In: Webb, B.W. (Ed.), Dissolved Loads of Rivers and Surface Water Quantity/Quality Relationships. IAHS Publication, pp. 173–192.
Meybeck, M., 2003. Global occurrence of major elements in rivers. In: Holland, H.D., Turekian, K.K. (Eds.), Treatise on Geochemistry. Elsevier, New York, pp. 207–223.
Millot, R., Gaillardet, J.É., Dupré, B., Allègre, C.J., 2003. Northern latitude chemical weathering rates: clues from the Mackenzie River Basin, Canada. Geochim. Cosmochim. Acta 67, 1305–1329.
Moon, S., Huh, Y., Zaitsev, A., 2009. Hydrochemistry of the Amur River: weathering in a Northern temperate basin. Aquat. Geochem. 15, 497–527.
Moquet, J.-S., Crave, A., Viers, J., Seyler, P., Armijos, E., Bourrel, L., Chavarri, E., Lagane, C., Laraque, A., Casimiro, W.S.L., Pombosa, R., Noriega, L., Vera, A., Guyot, J.-L., 2011. Chemical weathering and atmospheric/soil CO_2 uptake in the Andean and Foreland Amazon basins. Chem. Geol. 287, 1–26.
Négrel, P., Allègre, C.J., Dupré, B., Lewin, E., 1993. Erosion sources determined by inversion of major and trace element ratios and strontium isotopic ratios in river water: the Congo Basin case. Earth Planet. Sci. Lett. 120, 59–76.
Palmer, M.R., Edmond, J.M., 1992. Controls over the strontium isotope composition of river water. Geochim. Cosmochim. Acta 56, 2099–2111.
Qian, Z., 2007. Some Strategy Researches on Soil and Water Resources Allocation, Ecological and Environmental Protection and Sustainable Development in the Northeast China: Comprehensive Volume (in Chinese). Science Press, Beijing.
Qin, R., Wu, Y., Xu, Z., Xie, D., Zhang, C., 2013. Assessing the impact of natural and anthropogenic activities on groundwater quality in coastal alluvial aquifers of the lower Liaohe River Plain, NE China. Appl. Geochem. 31, 142–158.
Rai, S.K., Singh, S.K., Krishnaswami, S., 2010. Chemical weathering in the plain and peninsular sub-basins of the Ganga: impact on major ion chemistry and elemental fluxes. Geochim. Cosmochim. Acta 74, 2340–2355.
Raymo, M.E., Ruddiman, W.F., Froelich, P.N., 1988. Influence of late Cenozoic mountain building on ocean geochemical cycles. Geology 16, 649–653.
Raymond, P.A., Oh, N.-H., Turner, R.E., Broussard, W., 2008. Anthropogenically enhanced fluxes of water and carbon from the Mississippi River. Nature 451, 449–452.
Roy, S., Gaillardet, J., Allègre, C.J., 1999. Geochemistry of dissolved and suspended loads of the Seine River, France: anthropogenic impact, carbonate and silicate weathering. Geochim. Cosmochim. Acta 63, 1277–1292.
Shin, W.-J., Ryu, J.-S., Park, Y., Lee, K.-S., 2011. Chemical weathering and associated CO_2 consumption in six major river basins, South Korea. Geomorphology 129, 334–341.
SEPA (State Environmental Protection Administration of China), 1996. Report on the State of the Environment in China.
Song, Y., 2015. Staudy on '12th Five-year' plan of water pollution prevention and control of Liao River Basin. China Environmental Science Press, Beijing (in Chinese).
Tian, L., Lang, Y., Ding, H., Zhao, Z., Li, S., Hu, J., Zhang, Z., Liu, B., 2012. A study on the S isotope characters of Liao River Basin (in Chinese). The New Technology and New Methods of Isotope Geology and their Applications Xiamen.
Vengosh, A., Chivas, A.R., Starinsky, A., Kolodny, Y., Baozhen, Z., Pengxi, Z., 1995. Chemical and boron isotope compositions of non-marine brines from the Qaidam Basin, Qinghai, China. Chem. Geol. 120, 135–154.
Viers, J., Dupre, B., Braun, J.-J., Freydier, R., Greenberg, S., Ngoupayou, J., Nkamdjou, L., 2001. Evidence for non-conservative behaviour of chlorine in humid tropical environments. Aquat. Geochem. 7, 127–154.
Viers, J., Oliva, P., Dandurand, J.L., Dupré, B., Gaillardet, J., 2014. 7.6 – Chemical weathering rates, CO_2 consumption, and control parameters deduced from the chemical composition of rivers. In: Turekian, H.D.H.K. (Ed.), Treatise on Geochemistry. second ed. Elsevier, Oxford, pp. 175–194.
Wang, F., Yu, Y., Liu, C., Wang, B., Wang, Y., Guan, J., Mei, H., 2010. Dissolved silicate retention and transport in cascade reservoirs in Karst area, Southwest China. Sci. Total Environ. 408, 1667–1675.
Wang, W., Liu, H., Tang, D., Zhang, W., Lu, X., 1997. On the sources of acid rain at Fenghuang Mountain area in Liaoning Province (in Chinese). Res. Environ. Sci. 10, 22–26.
Wang, W., Xu, P., 2009. Research progress in precipitation chemistry in China (in Chinese). Prog. Chem. 21, 266–281.
White, A.F., Blum, A.E., 1995. Effects of climate on chemical_ weathering in watersheds. Geochim. Cosmochim. Acta 59, 1729–1747.
Wu, F.Y., Sun, D.Y., Li, H.M., Wang, X.L., 2001. The nature of basement beneath the Songliao Basin in NE China: geochemical and isotopic constraints. Phys. Chem. Earth Part A. 26, 793–803.
Wu, L., Huh, Y., Qin, J., Du, G., van Der Lee, S., 2005. Chemical weathering in the Upper Huang He (Yellow River) draining the eastern Qinghai-Tibet Plateau. Geochim. Cosmochim. Acta 69, 5279–5294.
Xia, B., LIu, Y., Sun, S., Zhang, J., 2009. Agricultural industry structure optimization and countermeasure in Dongliao river basin. Water Resour. Hydropower Northeast China 27, 3–5.
Xu, Z., Liu, C.-Q., 2007. Chemical weathering in the upper reaches of Xijiang River draining the Yunnan-Guizhou Plateau, Southwest China. Chem. Geol. 239, 83–95.
Xu, Z., Liu, C.-Q., 2010. Water geochemistry of the Xijiang basin rivers, South China: chemical weathering and CO_2 consumption. Appl. Geochem. 25, 1603–1614.
Yan, B., Song, X., Yan, M., Deng, W., Yan, D., 2000. Evolution trend of water in Liaohe river catchment (in Chinese). Bull. Soil Water Conserbatopm 20, 1–5.
Yang, J.-H., Wu, F.-Y., Chung, S.-L., Wilde, S.A., Chu, M.-F., 2004. Multiple sources for the origin of granites: geochemical and Nd/Sr isotopic evidence from the Gudaoling granite and its mafic enclaves, northeast China. Geochim. Cosmochim. Acta 68, 4469–4483.
Yang, J.-H., Wu, F.-Y., Chung, S.-L., Wilde, S.A., Chu, M.-F., 2006. A hybrid origin for the Qianshan A-type granite, northeast China: geochemical and Sr–Nd–Hf isotopic evidence. Lithos 89, 89–106.
Yue, F.-J., Li, S.-L., Liu, C.-Q., Zhao, Z.-Q., Hu, J., 2013. Using dual isotopes to evaluate sources and transformation of nitrogen in the Liao River, northeast China. Appl. Geochem. 36, 1–9.
Zhang, L., Song, X., Xia, J., Yuan, R., Zhang, Y., Liu, X., Han, D., 2011. Major element chemistry of the Huai River basin, China. Appl. Geochem. 26, 293–300.
Zhao, P., 2011. Countermeasure of development and utilization of water resources in Xiliao river basin (in Chinese). Water Resources Hydropower Northeast China 29, 31–32.

Further reading

SWRCMWR (Songliao Water Resources Commission), 1992. National Guideline of Liao River Basin (Revised Edition).